Journal of Applied Fluid Mechanics, Vol. 11, No. 2, pp. 433-446, 2018.
Available online at www.jafmonline.net, ISSN 1735-3572, EISSN 1735-3645.
DOI: 10.29252/jafm.11.02.27840

Numerical and Experimental Study of Separation Control by Boundary Layer Aspiration in a Highly-Loaded Axial Compressor Cascade

X. Mao, B. Liu† and F. Yuan

School of Power and Energy, Northwestern Polytechnical University 710072 Xi'an, Shaanxi, P. R. China

†*Corresponding Author Email: liubo704@nwpu.edu.cn*

(Received April 4, 2017; accepted November 8, 2017)

ABSTRACT

Both experiments and computations are performed and analyzed to investigate the effectiveness and mechanisms of different slotted aspiration schemes in controlling the separated flows in a highly-loaded axial compressor cascade. It is found that the boundary layer aspiration on the blade suction surface can improve the incidence characteristics of the airfoil within most of the incidence range except of the extremely high incidence and the profile loss coefficient is reduced remarkably as the aspirated massflow increases. The combined aspiration is the most effective scheme to control both the separated flow on the blade suction surface and the three-dimentional hub corner separation, and an improper design of aspiration would lead to a deterioration of the flow field. Different aspiration schemes have different effectiveness in controlling the flow separation, which leads to various influences on the blade loading and the diffusion abilities. The cascade incidence characteristics of different aspiration schemes show that the part-span aspiration scheme (SS1) located on the blade suction surface can only improve the overall flow field in very high incidences, while the other schemes can reduce the overall loss coefficient within almost the whole incidence range, especially for the combined aspiration scheme. There always exists a closed separation in the cascade when the boundary layer separation is not removed completely on the blade suction surface and in the hub corner. In addition, the type of critical point is affected by the spanwise static pressure gradient, which has significant effects on the cascade performance.

Keywords: Boundary layer separation; Aspiration; Three-dimensional corner separation; Critical point; Axial compressor cascade.

NOMENCLATURE AND ABBREVIATION

C	blade chord length
Cp	static pressure coefficient
h	blade height
i	flow incidence
Ma_1	inlet Mach number
P	local static pressure
P_1	inlet static pressure
P^*	local total pressure
P_1^*	inlet total pressure
t	blade pitch
y	pitch-wise distance from the SS
v	velocity
v_{fs}	free-stream velocity
w	local total pressure loss coefficient
$\overline{w}$	overall total pressure loss coefficient
β_s	blade stagger angle
β_{1k}	blade inlet angle
β_{2k}	blade outlet angle
δ	boundary layer thickness
δ^*	displacement thickness
ρ	density

Abbreviation

AFR Aspiration Flow Ratio
BLS Boundary Layer Separation

CA Combined Aspiration Scheme
EW End-Wall
EWA End Wall Aspiration Scheme
HP Horseshoe Vortex of Pressure Side Leg
HS Horseshoe Vortex of Suction Side Leg
LE Blade Leading Edge
SS Suction surface
SS1 Aspiration Scheme1 on the SS
SS2 Aspiration Scheme2 on the SS
TE Blade Trailing Edge

1. INTRODUCTION

Design trend for modern gas-turbine engine is to increase the thrust-to-weight ratio, which leads to a compressor design with higher aerodynamic loads and a reduction of number of blades and stages, so the prevention of flow separation becomes more and more challenging. The associated higher adverse pressure gradient increases the possibility of the boundary layer separation on the blade suction surface and the development of the three-dimensional (3D) hub corner separation. Therefore, it is needed to relieve or eliminate the flow separation by using some techniques to improve the aerodynamic performance of compressors (Hah *et al*. 1997; Lei 2006; Zhang *et al*. 2014; Beselt at al. 2014). As one of the effective methods to affect the flow separation, boundary layer aspiration attracts the attention from an increasing number of researchers.

Since 1950s, active flow control method of boundary layer aspiration has been explored extensively experimentally and theoretically to improve the compressor overall performance (Sinnettej *et al*. 1951; Costello *et al*. 1952). In 1971, Burger and Bogardus studied the effect of stator hub-slit aspiration on a high-speed compressor stage and found improvements on the compressor efficiency at several rotating speeds (Burger *et al*. 1971). Putting forward the concept of aspirated compressor in 1997, Kerrebrock *et al.* pointed that an improvement of flow turning and efficiency could be obtained via applying boundary layer aspiration at the position where the shock exists on the blade suction surface in a transonic compressor (Kerrebrock *et al*. 1997, 1998). In addition, Reijnen showed that boundary layer aspiration would be favorable to a reduction of flow deviation at blade exits and delaying rotating stall (Reijnen *et al*. 1997). Large amounts of work about boundary layer aspiration have been conducted by Massachusetts Institute of Technology (MIT) in cooperation with NASA Glenn Research Center since 1993, and an aspirated compressor design system was set up systematically. Both a low rotating speed stage with a pressure ratio of 1.6 at a rotor tip speed of 229m/s and a high rotating speed stage with a pressure ratio of 3.5 at a rotor tip speed of 457m/s were designed and successfully tested, which indicates that aspirated fan stage had a broad application prospect in the future (Schuler *et al*. 1998, 2000; Merchant at al. 2000; Kerrebrock er al. 2005). A two stage aspirated counter-rotating fan was also designed and tested with a design pressure ratio of 3:1 and adiabatic efficiency of 87% at design speed (Kirchner er al. 2002; Merchant *et al.* 2004; Onnée 2005). In addition, Dang *et al*. has also successfully redesigned a transonic rotor with an increase of efficiency about 1.4% by using aspiration (Dang *et al*. 2003). A numerical investigation of end-wall boundary layer removal on both the tip region of rotor and hub region of stator indicates that it was proved to give some control of local reverse flow, blockage and the associated loss generation when the boundary layer fluid was removed (Gümmer *et al*. 2008). An investigation of boundary layer aspiration on a low rotating speed stage based on the concept of an aspirated compressor by Qiang *et al*. shows that the method of boundary layer aspiration is effective and the 3D hub corner separation can be well controlled (Qiang *et al*. 2008). A non-standard aerodynamic design idea of highly-loaded supersonic or transonic axial flow compressors has been proposed by Hu *et al.* The aim of this design idea is to further increase the stage loads efficiently with boundary layer aspiration used only in the stator (Hu *et al*. 2013).

To gain a better insight into the nature and mechanisms of the technique of boundary layer aspiration, a number of studies have been carried out on the two-dimensional (2D) airfoils and 3D cascade with aspiration. Godard *et al*. conducted inverse design of the subsonic aspirated airfoil and obtained a profile with diffusion factor of 0.73 and turning angle of 60 degree with 1.1% of the inlet mass flow removed. The experiment shows a flow deflection of approximately 65 degree was achieved with an aspirated mass flow rate of 3.3% (Godard *et al.* 2008, 2012). and Song *et al*. performed extensive numerical studies on the effects of boundary layer aspiration on the performance of a compressor cascade with a large camber angle. They found that boundary layer aspiration is proved to be an effective approach to improve the cascade performance and it can further reduce the total pressure loss with combined aspiration slots on the blade suction surface (Chen *et al*. 2006; Song *et al.* 2006). Ding *et al*. carried out both experiments and numerical simulations

with aspiration holes on the blade suction surface in different positions. It is found that both side and middle aspirations on the blade suction surface can efficiently remove the low energy fluids to increase the cascade load capacity (Ding *et al.* 2013). Guo *et al*. also found that losses near both mid-span and end-wall can be reduced with aspiration slot on the blade suction surface, and the aspiration position plays a greater role in affecting the total pressure loss than the aspiration flow ratio (AFR) does. AFR is defined as the ratio of aspiration mass flow rate to the cascade inlet mass flow rate (Guo *et al.* 2010). Hubrich *et al.* studied a transonic annular cascade numerically and experimentally via boundary layer aspiration on the blade suction surface and found that the maximum pressure ratio and maximum diffusion could both be increased about 10% by sucking 20% of the inlet flow (Hubrich *et al*. 2004).

In addition to the loss associated with the boundary layer separation on the blade suction surface, high incidence also contributes to an increasing of the extent of 3D hub corner separation due to both the stream-wise and cross-passage pressure gradient, which will increase the blockage and loss production (Gbadebo *et al*. 2004). Therefore, the control of boundary layer separation on the blade suction surface must be accompanied by the end wall aspiration (EWA) to control the 3D hub corner separation. One of the earliest studies using EWA to control the 3D hub corner separation in compressor cascades was conducted by Peacock and the 3D hub corner separation was removed with an AFR of 0.6% (Peacock 1971). Since then, a number of researches have been conducted via EWA on the end-wall so as to gain a better control of the 3D hub corner separation by removing the secondary flow (Gbadebo *et al*. 2008; Liesner *et al*. 2010, 2013; Lemke *et al*. 2013; Chen et al. 2014, 2015). In addition, Cao et *al*. and Liu *et al.* evaluated the aspiration schemes by combining aspiration slots on both the blade suction surface and end-wall. With combined aspiration (CA), the separations in the cascade are almost removed completely (Cao *et al*. 2014; Liu *et al*. 2014).

According to the above statement, flow separations play an important role in the deterioration of compressor performance. In addition, it has been proved that the flow control technique of boundary layer aspiration is an effective approach to alleviate or remove the flow separations in comoressor and it can be successfully applied in the aspirated compressor stages. However, many of the existing researches on the boundary layer aspiration mainly concentrate on the influence of the slot position, geometrical shape or AFR on the separation control and the stage overall performance. The previous works also mainly focused on a single flow condition near design using boundary layer aspiration in cascades. In addition, the current paper's cascade has separated flows both on the blade suction surface along the whole blade span and 3D hub corner separation, while the literatures about the influence of different slotted schemes and combined control scheme on the separated flows are rare. Therefore, numerical studies of separation control together with experiments have been conducted in a highly-loaded compressor cascade under off-design flow conditions by applying different aspiration schemes in the current paper.

2. INVESTIGATED COMPRESSOR CASCADE AND NUMERICAL METHOD

2.1 Cascade Description

The investigated original cascade is composed of nine blades, and the cascade design parameters and test conditions at the aerodynamic design point are listed in Table 1. The blade airfoil is described as multi-circular-arc (MCA). The maximum relative thickness is 0.08 at the maximum thickness position of 0.61 blade chord. In the current paper, the Mach number and incidence of incoming flow are about 0.55 and 5 degree respectively for the different aspiration sschemes in both the experiments and computations. Fig. 1 shows the cascade configuration.

Table 1 Cascade design parameters

Parameter	Variable	Value	Unit
Number of blades	-	9	*[-]*
Blade chord length	C	63	*mm*
Blade height	h	100	*mm*
Blade pitch	t	37.95	*mm*
Aspect ratio	h/C	1.59	*[-]*
Blade solidity	t/C	1.66	*[-]*
Blade stagger angle	β_s	15.4	*degree*
Blade inlet angle	β_{1k}	40.17	*degree*
Blade outlet angle	β_{2k}	-13.21	*degree*
Inlet Mach number	Ma_1	0.55	*[-]*
2D diffusion factor	DF	0.46	*[-]*

2.2 Computational Methodology

3D numerical simulation software of EURANUS from NUMECA International was used to conduct the computations on structured non-orthogonal multi-block grids. An explicit four-order Runge-Kutta scheme was used for temporal discretization. The discretization in space was based on a second order cell-centered explicit finite volume scheme

with four-order artificial dissipation. One equation turbulence model of Spalart and Almaras (S-A) (Spalart *et al*. 1992) was employed to estimate the eddy viscosity. Absolute total pressure, total temperature and inlet flow angle were presented at the inlet boundary of the blade passage. The average static pressure at the outlet condition of the blade passage was adjusted based on the desired flow rate. The desired aspirated mass flow rates was set on the outlet condition of the aspiration slot.

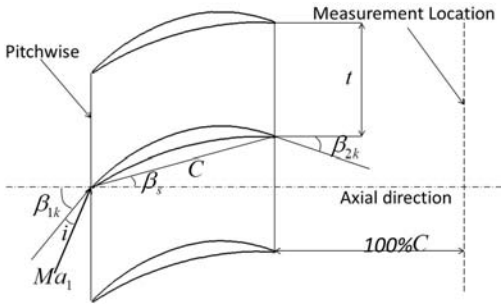

Fig. 1. 2D cascade configuration.

The computational structured mesh of O4H type of the blade passage was generated by AUTOGRID5 from NUMECA international. The grid of the aspiration slots is a structured H grid created by a structured generator of IGG. The grids of the blade passage and aspiration slots were connected to each other by full non-matching connection technology, a technique which allows arbitrarily connecting grid blocks of different grid topologies or point numbers to each other without significant numerical interpolation losses. The total mesh number of the main blade passage and slot were about 1.0 and 0.1 million separately. The minimum grid spacing on the solid wall was 5×10^{-6} m to evaluate the viscous fluxes at the walls by applying the no-slip and adiabatic conditions. The grid near the blade suction surface (SS) and end-wall (EW) is shown in Fig. 2.

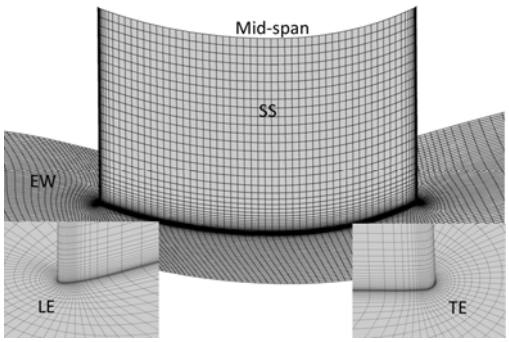

Fig. 2. Grid near the blade suction surface and end-wall.

3. Aspiration Schemes Design and Experimental Facilities

3.1 Aspiration Schemes Design

Computations of the basic flow were conducted first to support an appropriate deign of the aspiration schemes. Numerical results of the flow structures in the original cascade are shown in Fig. 3. Since the flow in the cascade is symmetric, consideration of one side is sufficient. It can be found that there are separations both on the blade suction surface and in the hub corner. There is boundary layer separation (BLS) at about 84% axial chord on the blade suction surface at mid-span, and the separation line is more and more close to the blade leading edge at lower span due to the influence of secondary flow from the end-wall. The streamlines correspond to the suction side and pressure side legs of horseshoe vortex at leading edge are colored with red and green respectively. Additionally, the 3D streamlines released from two different positions within the end-wall boundary layer at about mid-pitch are also depicted in Fig. 3, i.e., blue streamlines (a quarter of boundary layer thickness away from the end-wall) and magenta streamlines (a half of boundary layer thickness away from the end-wall).

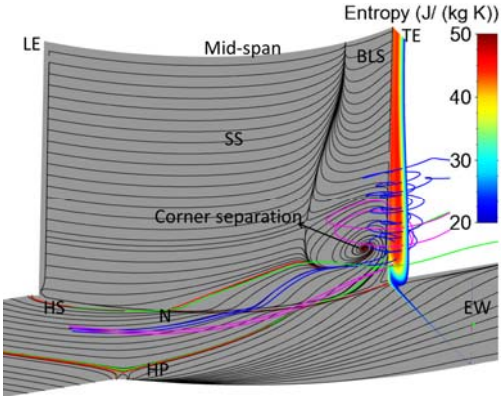

Fig. 3. Computed 3D hub corner separated flow structures and detailed limiting streamlines on blade suction surface and end-wall.

One can see that the suction side leg of horseshoe vortex, which starts from the leading edge (LE) stagnation point, intersects with the blade suction surface at about 25% axial chord (point N) due to the influence of cross-passage pressure gradient. From the point of N separation line on the blade suction surface originates and migrates from hub to mid-span, which plays a significant role in the formation of the 3D hub corner separation. The streamlines corresponding to the pressure side leg of horseshoe vortex also intersect with the suction

surface of the neighboring blade and contribute to the formation of the 3D hub corner separation. The blue streamlines released from the lower location within boundary layer are driven earlier toward the blade suction surface by circumferential pressure gradient and surrounded by the magenta streamlines which has a higher stream-wise momentum. Therefore, the 3D hub corner separated region is filled with separated fluids from both the blade suction surface and end-wall.

In order to give consideration to controlling the separated flows, three kinds of slotted schemes were designed in the experiments, i.e., two suction surface slotted schemes and one end-wall slotted scheme shown as Fig. 4. It is widely accepted that the best position of boundary layer aspiration on the blade suction surface is near the separation onset point for subsonic compressor blade. In order to give consideration to the hub corner flows, the two slots on the blade suction surface are along spanwise and at about 68% axial chord with a width of about 2.4% blade chord. In the first case defined as SS1 (part-span aspiration), a rectangular slot is at the middle of the blade span with a height of 60 mm. Another slot defined as SS2 (full-span aspiration) is set up along the whole blade span. The end-wall slot scheme defined as EWA is located at about 2.4% blade chord away from the blade suction surface with a width of about 2.4% blade chord, and it runs parallel to the blade suction surface from about 17% to 100% axial chord in order to cover the point of N.

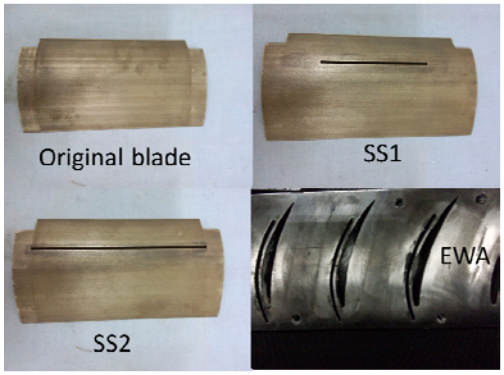

Fig. 4. Pictures of different slotted schemes.

3.2 Experimental Setup

The experiments described in this paper were performed in a high subsonic cascade wind tunnel at the National Defense Aerodynamics Laboratory of Airfoil and Cascade in Northwestern Polytechnical University in Xi'an, and a large number of experiments have been conducted successfully in the cascade wind tunnel, which gives us confidence in the use of the experimental facilities and systems. Since the cascade was symmetric with respect to the mid-span, only half of the blade was investigated. The flow parameters were measured with a five-hole probe located one true chord downstream of the cascade trailing edge at six spanwise locations (5%, 10%, 20%, 30%, 40% and 50% blade height). The aspirated blade has a hollow structure. The five original blades in the center of the cascade were replaced with aspirated blades in the suction surface slotted schemes. The slots were also set up on the end-wall corresponding the middle five blades in the slotted scheme of EWA shown in Fig. 5. The low-energy gas of the separated fluids was sucked from the slot to the cavity of the blades or end-wall chamber and then flowed outside of the cascade. A flow-meter was used to control the AFR.

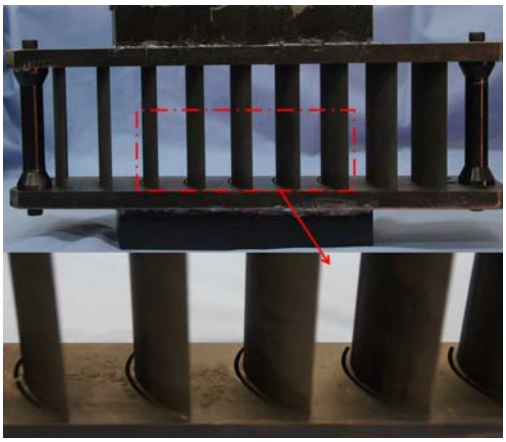

Fig. 5. Picture of the slotted scheme of EWA.

To ensure the validity of the experimental results, the periodicity of the flow in different blade passages was checked before the experiments and the results showed that the flow in different blade passages showed a good periodicity. The difference of total pressure loss between two ajacent blade passages is less than 5%. Thus, only one flow passage was studied in view of the periodicity of the different blade passages. Additionally, the experiments of typical working conditions were repeated two or three times to guarantee the consistency in measurement.

4. Results And Discussion

4.1 Numerical Method Evaluation with Experiments

In order to guarantee the reliability of the computational results, the comparisons of the numerical and experimental results are made by the pitch-averaged total pressure loss coefficient (w)

and static pressure coefficient (*Cp*). Figure 6 compares the *Cp* results of the experiments and numerical simulations for the original cascade at mid-span. The agreement between the experimental and numerical results is good except at about 70% axial chord on the suction surface. The loss coefficient on measurement plane at the incidences of 0.5° and 5.0° is plotted in Fig. 7. It can be seen that the loss distribution is satisfactorily captured. Although there are some deviations between the numerical and experimental results, the overall trend of the simulations fits well with the experimental data. Therefore, the numerical method used in current paper is appropriate for analyzing the aerodynamic performance of the highly-loaded compressor cascade. Additionally, the good agreement between numerical and experimental results in the following sections also gives us confidence in the use of this numerical method.

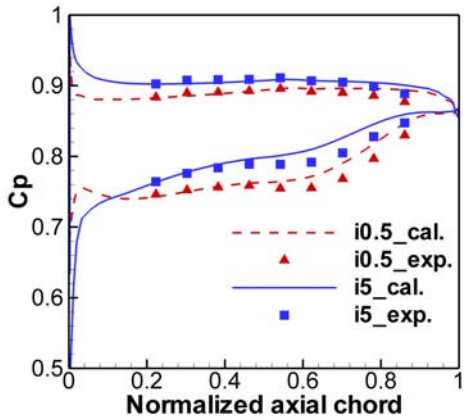

Fig. 6. *Cp* distributions of numerical and experimental results of the original cascade at mid-span.

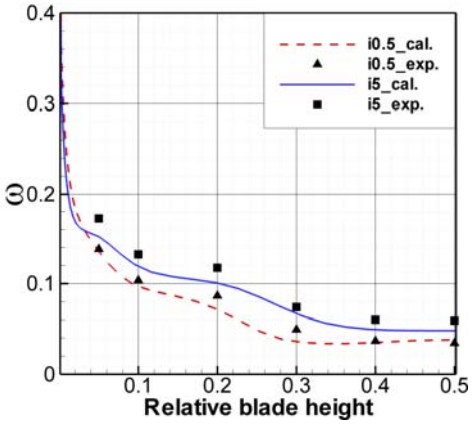

Fig. 7. Spanwise distribution of pitch-averaged total loss coefficient.

4.2 The Influence of the Slotted Scheme of SS1

The experimentally measured change in profile loss coefficient at mid-span with AFR together with the numerical results is shown in Fig. 8. It is found that boundary layer aspiration can reduce the airfoil loss coefficient remarkably. The loss coefficient is about 0.0881 with the AFR of 0.0 % at an incidence of 5°. As the aspiration rate increases, the loss coefficient dropped significantly. With an AFR of about 1.0 %, the loss coefficient reduced to about 0.0257. In addition, the numerical prediction agrees well with the experimental measurement at higher AFR. While the loss coefficient is lower for the experimental results at the AFR of 0.0 %, which indicates that the loss production due to the influence of the aspiration slot on the main flow is over-predicted by the numerical method at the AFR of 0.0%.

The profile loss coefficient versus incidence behaviors of the SS1 cascade at an AFR of about 1.0% is compared with the original cascade together with the numerical results in Fig. 9. The experimental results show that boundary layer aspiration can improve the incidence characteristics of the airfoil within most of the incidence range except of the very high incidence. At the very high incidence of 10°, boundary layer aspiration is found to increase the mid-span profile loss coefficient. For these cases, the separation on the blade suction surface has been highly serious with the onset point of separation moving forward and the migration of low energy fluids from the end-wall to mid-span also aggravates. Therefore, the boundary layer aspiration already cannot control the separation on the blade suction surface effectively when the aspiration slot is at the region of fully developed separation. However, the loss coefficient in the simulations is found to be reduced in the whole incidence range, which indicates that the numerical method is needed to be further improved at very high incidences. Additionally, the experimental and numerical data show very good agreement at most incidences.

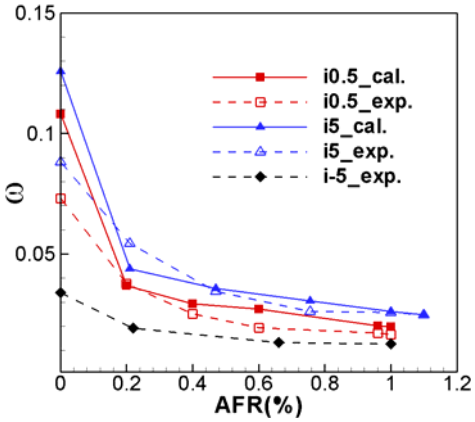

Fig. 8. Bleed characteristics with varying incidence and AFR.

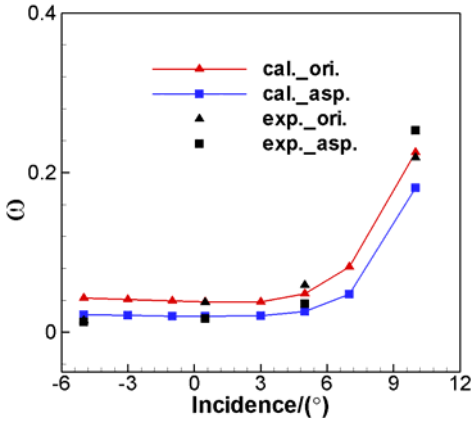

Fig. 9. Variation of airfoil loss with incidence at the AFR of about 1.0%.

In order to assess the effect of aspiration scheme of SS1 on the cascade performance, the spanwise distributions of pitch-averaged loss coefficient at the measurement plane are presented in Fig. 10. Both the measured and computed results show a reduction of loss coefficient from about 30% to 50% blade span when the aspiration scheme of SS1 was applied. It can also be seen that the increase of loss coefficient extends from the end-wall to about 30% blade span, which indicates that an improper location of aspiration would lead to a deterioration of the flow field.

The limiting streamlines and the contours of Cp on the blade suction surface for the original cascade and SS1 (AFR=1.0%) are depicted in Fig. 11. The apparent critical points are also marked in the figure to view the change of flow pattern and vortex structure. One can see that there are two separation lines of S1-N1 and S1-N2 starting from a saddle point of S1. They end at the nodal point of N1 and spiral point of N2 respectively, and a so-called concentrated shedding vortex is formed at the spiral point of N2 at about 7.5% blade span (Wang 1972). This is the typical of saddle point-spiral (nodal) point separation that indicates a distinct forbidden zone exists in the flow, and it belongs to a closed separation. In addition, the loss coefficient is increased when the saddle point-spiral point separation is evolved from the saddle point-nodal point separation due to the effect of mixing process from the concentrated shedding vortex (Lighthill 1963; Kang 1993; Zhang *et al*. 2007; Sachdeva *et al*. 2011).

After the aspiration of SS1, the flow fields around mid-span are improved remarkably, and the separation region at mid-span is almost removed completely which leads to the increase of the static pressure near the blade trailing edge. However, the separation area in the hub corner increases. As a result, the saddle point of S1 from which the separation lines of S1-N1 and S1-N2 originate moves upstream. It is interesting to note that the spiral point of N2 in the original cascade has degenerated into a nodal point, which means the disappearance of the concentrated shedding vortex at about 7.5% blade span. Due to the increase of static pressure around mid-span at the blade trailing edge, the spanwise pressure gradient also goes up from about 20% to 30% blade span shown as Fig. 12. Therefore, a new spiral point of N1 corresponding to the origination point of the concentrated shedding vortex at about 25.6% is generated, which shows that an increase of spanwise pressure gradient would contribute to the formation of concentrated shedding vortex. Therefore, the slotted schemes should be chosen properly to avoid introducing high pressure gradient along the blade span. Although the closed separation type keeps unchanged, the separation area in the hub corner increases. Thus, the loss coefficient goes up at lower blade span shown as Fig. 10. In addition, the moving up of the originating location of concentrated shedding vortex also increases the mixing loss within a larger range of blade span compared with the original cascade.

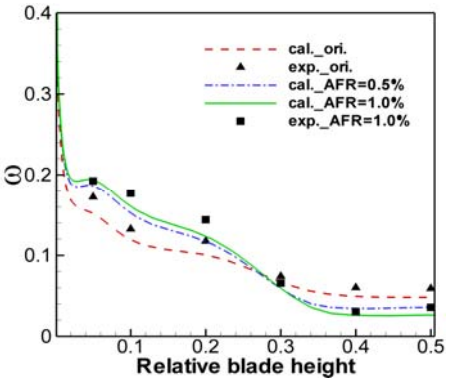

Fig. 10. Spanwise distribution of pitch-averaged total loss coefficient with scheme of SS1.

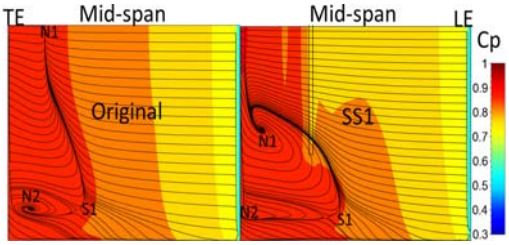

Fig. 11. Limiting streamlines of original cascade and SS1.

4.3 The Influence of the Slotted Scheme of SS2

From the analyses above, the aspiration scheme of SS1 can only effectively improve the performance

near the mid-span of the cascade resulting in the deterioration of the flow in the hub corner. Therefore, another aspiration scheme of SS2 is investigated to mitigate the 3D hub corner separation compared to the scheme of SS1.

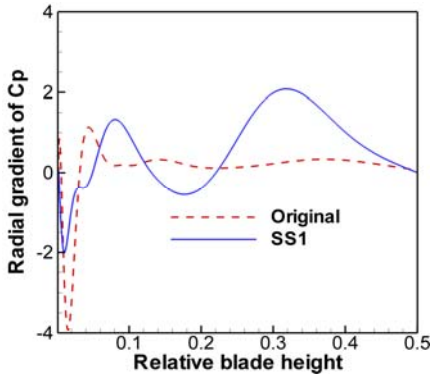

Fig. 12. Spanwise distribution of radial pressure gradient near the suction surface at the blade trailing edge.

Figure 13 shows the spanwise distributions of the loss coefficient at the measurement plane. It clearly shows a reduced loss coefficient along the whole blade span after the aspiration of SS2. However, the experimental results show a more remarkable reduction of the loss coefficient at lower blade span than the mid-span. For the aspiration structure used in the experiments, the low-energy separated fluids were sucked from the slot to the cavity of the blades and then from the end-wall chamber on both sides to the outside of the cascade. Therefore, there are spanwise differences in the efficacy of the applied aspiration control exhibited between the experimental cascade and computations, i.e., the aspirated control is more effective near the end-wall than mid-span, which leads to the different spanwise distribution of the loss coefficient in the experimental results from the numerical simulations.

Figure 14 shows the limiting streamlines together with the contours of Cp on the blade suction surface for the original cascade and SS2 (AFR=1.0%). It can be seen that the flow fields along the whole blade span are improved significantly. Although there still exists boundary layer separation at the blade trailing edge around mid-span, the separation area in hub corner reduces remarkably compared with the scheme of SS1. After the aspiration of SS2, only one separation line of S1-N1 is remained on the blade suction surface. The saddle point of S1 from which the separation line of S1-N1 originates moves downstream to the blade trailing edge and it is more adjacent to the end-wall. In addition, the spiral point in the hub corner also disappears which indicates the vanishing of the concentrated shedding vortex. Although the separation type is still closed separation, the weak saddle point and disappearance of the spiral point contribute to the intensity reduction of the blade trailing edge shedding vortex and corresponding loss coefficient.

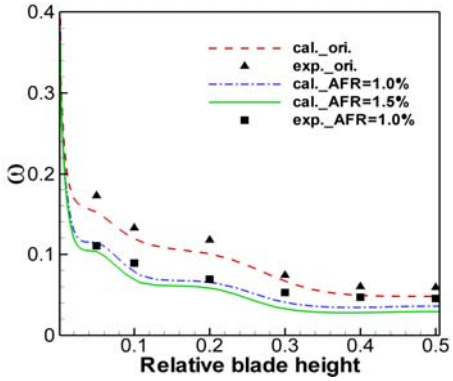

Fig. 13. Spanwise distribution of pitch-averaged total loss coefficient with scheme of SS2.

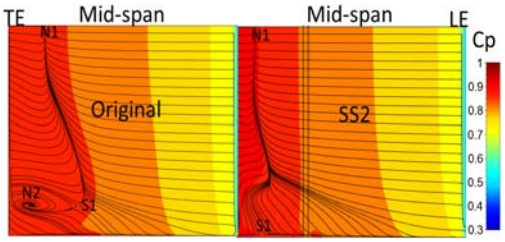

Fig. 14. Limiting streamlines of original cascade and SS2.

4.4 The Influence of the Slotted Scheme on the End-Wall

The 3D hub corner separation is the result of an interaction between the separated flow on the blade suction surface and the secondary flow from the end-wall. Although the scheme of SS2 can effectively reduce the separation on the blade suction surface and to some extent mitigate the low energy fluids from end-wall, there are still streamlines rising from the end-wall to the upper blade span shown as Fig. 14. Therefore, a slotted scheme of EWA is studied to further improve the flow field in the hub corner.

The spanwise distributions of loss coefficient at the measurement plane are shown in Fig. 15. One can see that the loss coefficient at lower blade span decreases with the increasing of the AFR, while the loss coefficient around mid-span increases slightly for the reason that the reduction of blockage in the hub corner leads to a decrease of stream-tube convergence caused by 3D hub corner separation. Therefore, the onset point of boundary layer

separation moves forward and leads to a thickening of the boundary layer separation in the mid-span region. It is also found that the end-wall slot has a significant impact on the main flow at the AFR of 0.0% in the computations, which leads to a remarkable increase of the loss coefficient from the end-wall to about 40% blade span. The experimental results show a more obvious reduction of loss coefficient than the numerical results with the AFR of about 0.67%, however, the effectiveness becomes obvious as the AFR increases to about 1.0% for the computational results. Therefore, there exists a critical AFR for the slotted scheme of EWA to function effectively. Because of the limitation of the aspiration system the experimental result of the loss coefficient at the AFR of about 1.0% was not obtained.

Figure 16 shows the limiting streamlines together with the contours of Cp on the blade suction surface for the original cascade and EWA with different AFR. It can be seen that the separation area of 3D hub corner separation increases remarkably at the AFR of 0.0% which is consistent with the increasing of the loss coefficient. In addition, the number of critical points also increases which shows the blockage of the separated region is increased (Gbadebo *et al*. 2004). The flow pattern on the blade suction surface for EWA is almost the same as the original except that the spiral point of N2 in the original cascade has degenerated into a nodal point at the AFR of about 0.67%, which means the disappearance of the concentrated shedding vortex. When the AFR is increased to about 1.0%, the 3D hub corner separation is removed completely and there only exists the boundary layer separation on the suction surface at blade trailing edge. The separation type is still a closed separation with a weak saddle point and two nodal points mainly due to the boundary layer separation at the blade trailing edge. Therefore, the aspiration on the end-wall is an effective method to control the 3D hub corner separation.

4.5 The Influence of the Combined Slotted Scheme of CA

Among the single slotted schemes discussed above, it is found that the scheme of SS2 can effectively reduce the separation on the blade suction surface and to some extent mitigate the 3D hub corner separation. The aspiration scheme of EWA can effectively remove the rising of low energy fluids from the end-wall. Therefore, a combined aspiration scheme of CA is explored numerically to further improve the flow field. The slot in the scheme of EWA is implemented based on the scheme of SS2. The AFR of about 1.2% and 1.0% is therefore given for the slot on the blade suction surface and the slot on the end-wall respectively in the scheme of CA.

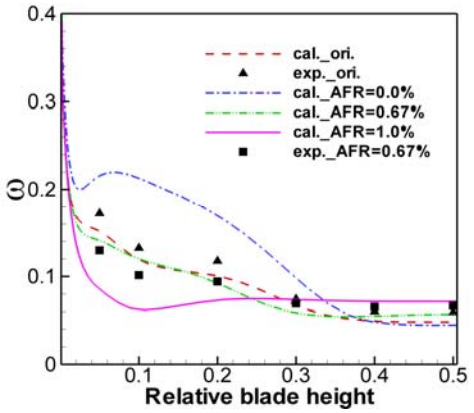

Fig. 15. Spanwise distribution of pitch-averaged total loss coefficient with scheme of EWA.

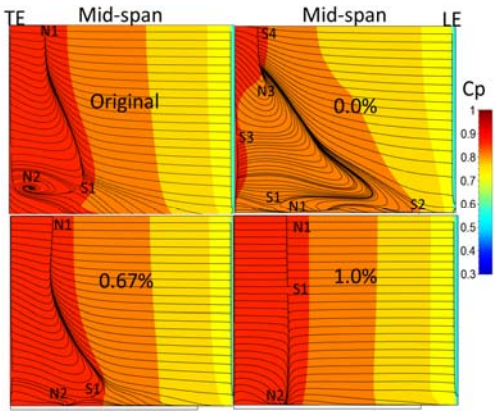

Fig. 16. Limiting streamlines of original cascade and EWA with different AFR.

The limiting streamlines together with the contours of Cp on the blade suction surface for the original cascade and CA are presented in Fig. 17. It can be seen that the limiting streamlines on the blade suction surface are improved significantly after the aspiration. The boundary layer separation at the blade trailing edge is reduced remarkably along the whole blade span, and the 3D hub corner separation is almost completely removed. The separation type is still closed separation after the aspiration of CA. Therefore, it is concluded that there always exists a closed separation in the cascade when the boundary layer separation is not removed completely at the blade trailing edge on the blade suction surface and in the hub corner. In addition, there does not exist spiral points corresponding to the concentrated shedding vortex because of the uniform pressure gradient after the aspiration. Figure 18 shows the entropy contours of different aspiration schemes at the measurement plane. One can see that the

combined aspiration scheme of CA is more effective than the single slotted schemes of SS2 and EWA. The distribution of entropy at the blade trailing edge also indicates the flow field after the cascade is more uniform.

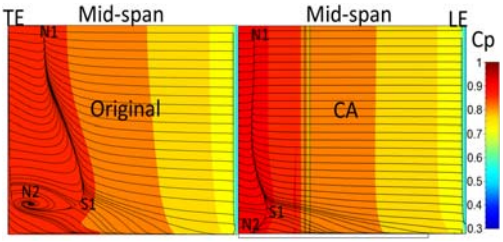

Fig. 17. Limiting streamlines of original cascade and CA.

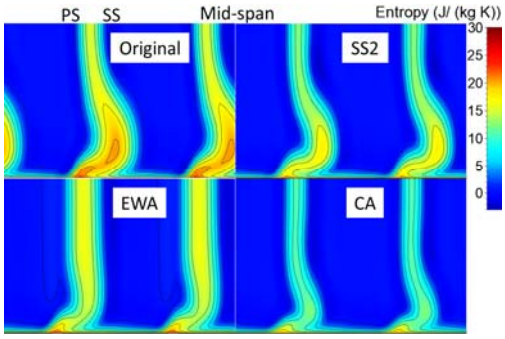

Fig. 18. Entropy contours of different aspiration schemes.

Figure 19 depicts the detailed static pressure coefficient distribution on blade surfaces at mid-span and 15% blade span. It is found that the aspiration of SS1 leads to an increase of the blade loading from the front of the slot position, and the pressure near the blade trailing edge goes up at mid-span. While it achieves neither noticeable increase in diffusion nor any rise of blade loading near the end-wall. Therefore, the scheme of SS1 can only influence the blade loading of span at which the suction slot exists, which is consistent with the results in Fig. 11. Both the diffusion ability and static pressure at the blade trailing edge along the whole blade span are improved significantly after the aspiration of SS2. The results of increased blade loading along the whole blade span from the front of the slot position can also be observed. However, the scheme of EWA can only improve both the diffusion ability and blade loading near the end-wall, which leads to a slight reduction of the blade loading around the mid-span. The scheme of CA can remarkably improve the blade loading and diffusion ability at the whole blade span from the front of the suction surface slot position, and the static pressure at the blade trailing edge is higher than other aspiration schemes. Therefore, the combined aspiration scheme is the most effective scheme to control the separated fluids both on the blade suction surface and in the hub corner.

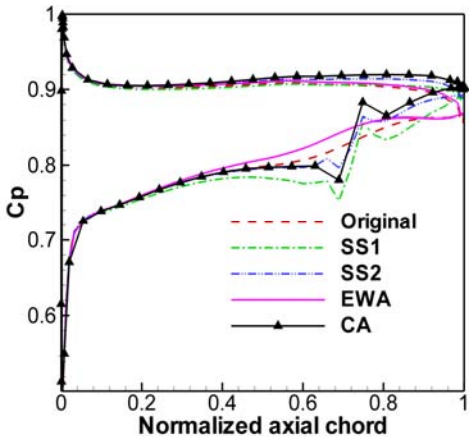

(a) Mid-span

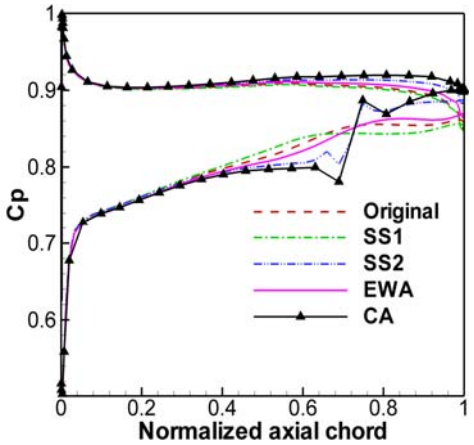

(b) 15% span

Fig. 19. Static pressure coefficient distributions at mid-span and 15% blade span.

The concept of relative displacement thickness was proposed by Gbadebo to estimate the thickness of the 3D separated layer perpendicular to the blade suction surface at the trailing edge (Gbadebo *et al.* 2004). It is the displacement thickness at other spanwise locations minus that at the mid-span. It can be normalized as a fraction of the blade chord as

$$\{\delta^*(r)\text{-}\delta_{mid}{}^*\}/C \tag{1}$$

The displacement thickness is given as

$$\delta^*(r)=\int_0^{\delta}[1-\frac{\rho v(r,y)}{\rho_{fs}v_{fs}}]\,dy \tag{2}$$

They are used here to judge the variation of boundary layer separation on the blade suction surface and the 3D hub corner separation in the different aspiration schemes. It should be

mentioned that there does not allow a clear edge of boundary layer on the blade suction surface until some distance from the end-wall. The local velocity at mid-pitch is used to approximate the free-stream velocity. Since there also exists boundary layer separation on the blade suction surface, and its extension is also influenced remarkably by the different aspiration schemes, therefore, the spanwise distribution of the normalized displacement thickness $\delta^*(r)$ is also presented in Fig. 21 together with the spanwise distribution of the relative displacement thickness in Fig. 20.

One can see that from the Fig. 20, all aspiration schemes except of SS1 are able to reduce the thickness of the 3D hub corner separation when compared with the original cascade. EWA is the most effective scheme to control the 3D hub corner separation. After aspiration of the scheme of SS1, the extent of 3D hub corner separation is increased dramatically. Figure 21 shows that the displacement thickness of the boundary layer separation on the blade suction surface near the mid-span reduces remarkably after the aspiration of SS1. The scheme of CA decreases both the boundary layer separation on the suction surface and the 3D hub corner separation significantly. Although the scheme of EWA reduces the extent of the 3D hub corner separation effectively, boundary layer separation on the blade suction surface is increased remarkably. Therefore, it is suggested to use the combined aspiration scheme of CA to control the separated fluids when there are both boundary layer separation on the blade suction surface and 3D hub corner separation.

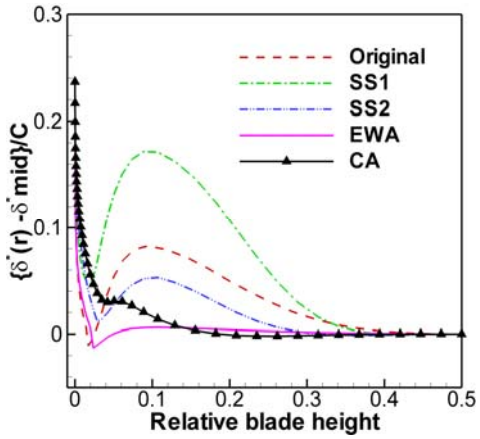

Fig. 20. Computed spanwise distribution of the normalized relative displacement thickness of the 3D hub corner separation at the blade trailing edge.

The flow in the 3D linear cascade can reflect the flow fields in the stator to some extent. In order to provide reference for better application of the aspiration schemes, the overall total pressure loss coefficient $\overline{w}$ obtained by integrating the loss profiles over the whole blade span is investigated with varying incidence.

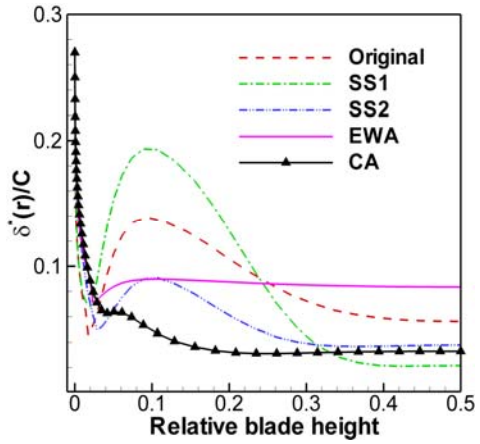

Fig. 21. Computed spanwise distribution of the normalized displacement thickness of the boundary layer separation at the blade trailing edge.

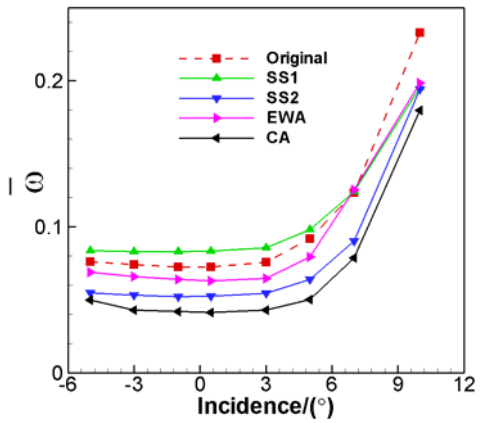

Fig. 22. Incidence characteristics of the cascade under different aspiration schemes.

Figure 22 shows the incidence characteristics for the different aspiration schemes. The results show that the scheme of SS1 can improve the overall flow field only in very high incidences, while the other schemes can reduce the overall loss coefficient within almost the whole incidence range, especially for the schemes of CA. At the same of AFR, the aspiration scheme of SS2 is more effective than the scheme of EWA. The overall loss in the scheme of SS1 is lower than that in original cascade from the incidence of 7°. It shows that the boundary layer separation on the suction surface is more predominant at the very high incidence and it is more effective to control the separation by aspiration slot on the blade suction surface. The overall loss in scheme of EWA is the same as that in original cascade at the incidence of 7°. It may be

the reason that the optimal location of the aspiration slot and critical AFR are various at different incidences.

5. CONCLUSIONS

The goals of present paper are to investigate the effectiveness and mechanisms of different slotted aspiration schemes in controlling the separated fluids in a highly-loaded compressor cascade. The findings can be summarized as follows.

1. The experimental results show that the profile loss coefficient is reduced remarkably as the AFR increases. Boundary layer aspiration on the blade suction surface can improve the incidence characteristics of the airfoil within most of the incidence range except of the very high incidence.

2. The part-span aspiration scheme of SS1 can only effectively improve the performance near the mid-span of cascade resulting in the deterioration of the flow in the hub corner, which indicates that an improper location of aspiration would lead to a deterioration of the flow field. The aspiration on the end-wall is an effective method to control the 3D hub corner separation resulting in an increase of boundary layer separation on the blade suction surface and there exists a critical AFR for the slotted scheme of EWA to function effectively. The aspiration scheme of CA is the most effective choice to control both the separated fluids on the blade suction surface and the 3D hub corner separation.

3. Different aspiration schemes have various influences on the blade loading and the diffusion abilities, and the scheme of CA can remarkably improve the blade loading and diffusion ability at the whole blade span. There always exists a closed separation in the cascade when the separation is not removed completely on the blade suction surface and in the hub corner. The type of critical point is affected by the spanwise static pressure gradient, which has significant effects on the cascade performance.

4. The cascade incidence characteristics of different aspiration schemes show that the scheme of SS1 can only improve the overall flow field in very high incidences, while the other schemes can reduce the overall loss coefficient within almost the whole incidence range, especially for the scheme of CA. After the aspiration of CA, the flow field after the cascade becomes more uniform.

ACKNOWLEDGEMENTS

This paper is supported by National Natural Science Foundation of China (Project No: 51676162) and Collaborative Innovation Center of Advanced Aero-Engine in Beijing, these supports are gratefully acknowledged.

REFERENCES

Beselt, C., M. Eck and D. Peitsch (2014). Three-dimensional flow field in highly loaded compressor cascade. *Journal of Turbomachinery* 136(10), 101007.

Burger, G. and G. Bogardus (1971). Single-stage evaluation of highly-loaded high-Mach-number compressor stages IV.Data and performance of hub-slit suction stator. *NASACR-120802*.

Cao, Z., B. Liu and T. Zhang (2014). Control of separations in a highly loaded diffusion cascade by tailored boundary layer suction. *Proceedings of the Institution of Mechanical Engineers, Part C: Journal of Mechanical Engineering Science* 228(8),1363-1374.

Chen, F., Y. Song, H. Chen and Z. Wang (2006). Effects of boundary layer suction on the performance of compressor cascades. *ASME GT2006-90082*.

Chen, P., W. Qiao, K. Liesner and R. Meyer (2014). Location effect of boundary layer suction on compressor hub-corner separation. *ASME GT2014-25043*.

Chen, P., W. Qiao, K. Liesner and R. Meyer (2015). Effect of Segment Endwall Boundary Layer Suction on Compressor 3D Corner Separation. *ASME GT2015-42024*.

Costello, G., R. Cummings and G. Serovy (1952). Experimental Investigation of Axial Flow Compressor Stator Blades Designed to Obtain High Turning by Means of Boundary-Layer Suction. *NACA RM E52D18*.

Dang, T., M. Van Rooij and L. Larosiliere (2003). Design of aspirated compressor blades using three-dimensional inverse method. *ASME GT2003-38492*.

Ding, J., S. Chen, H. Xu, S. Sun, and S. Wang (2013). Control of flow separations in compressor cascade by boundary layer suction holes in suction surface. *ASME GT2013-94723*.

Gbadebo, S., N. Cumpsty and T. Hynes (2004). Three-dimensional separations in axial

compressors. *ASME GT2004-53617*.

Gbadebo, S., N. Cumpsty and T. Hynes (2008). Control of three-dimensional separations in axial compressors by tailored boundary layer suction. Journal of turbomachinery,130(1), 011004.

Godard, A., A. Fourmaux, S. Burguburu and F. Lebœuf (2008). Design method of a subsonic aspirated cascade. *ASME GT2008-50835*.

Godard, A., A. Fourmaux, S. Burguburu and F. Lebœuf (2012). Experimental and numerical study of a subsonic aspirated cascade. *ASME GT2012-69011*.

Gümmer, V., M. Goller and M. Swoboda (2008). Numerical investigation of end wall boundary layer removal on highly loaded axial compressor blade rows. *Journal of Turbomachinery* 130(1), 011015.

Guo, S., C. Shaowen, S. Yanping, S. Yufei and C. Fu (2010). Effects of boundary layer suction on aerodynamic performance in a high-load compressor cascade. *Chinese Journal of Aeronautics*, 23(2), 179-186.

Hah, C. and J. Loellbach (1997). Development of hub corner stall and its influence on the performance of axial compressor blade rows. *ASME 97-GT-42.*

Hu, Y., W. Songtao, Z. Longxing and D. Jun (2013). Aerodynamic design of a highly loaded supersonic aspirated axial flow compressor stage. *Proceedings of the Institution of Mechanical Engineers, Part A: Journal of Power and Energy* 228(3), 241-254.

Hubrich, K., A. Bolcs and P. Ott (2004). Boundary Layer Suction Via a Slot in a Transonic Compressor: Numerical Parameter Study and First Experiments. *ASME GT2004-53758*.

Kang, S (1993). Investigation on the three dimensional flow within a compressor cascade with and without tip clearance. *Brussels: Vrije University Brussels*.

Kerrebrock, J., D. Reijnan, S. Ziminsky and L.Smilg (1997). Aspirated compressors. *ASME No. 97-GT-525*.

Kerrebrock, J., J. Adamczyk and E. Braunscheidel (2005). Experimental Investigation of a High Pressure Ratio Aspirated Fan Stage. *Journal of turbomachinery* 127(1), 43-51.

Kerrobrock, J., M. Drela, A. Merchant and B. Schuler (1998). A family of designs for aspirated compressors. *ASME 98-GT-196.*

Kirchner, J (2002). Aerodynamic design of an aspirated counter-rotating compressor. *Ph. D. thesis, the Massachusetts Institute of Technology, Boston, USA.*

Lei, V. (2006). A simple criterion for three-dimensional flow separation in axial compressors. *Ph. D. thesis, the Massachusetts Institute of Technology, Boston, USA.*

Lemke, M., C. Gmelin and F. Thiele (2013). Simulations of a compressor cascade with steady secondary flow suction. *New Results in Numerical and Experimental Fluid Mechanics VIII. Springer Berlin Heidelberg* 549-556.

Liesner, K and R. Meyer (2013). Evaluation of Passive and Active Secondary Flow Control in a High Speed Compressor Cascade with Different Measurement Techniques. *New Results in Numerical and Experimental Fluid Mechanics VIII. Springer Berlin Heidelberg* 125-133.

Liesner, K., R. Meyer, M. Lemke, C. Gmelin and F. Thiele (2010). On the efficiency of secondary flow suction in a compressor cascade. *ASME GT2010-22336*.

Lighthill, M (1963). Attachment and separation in three-dimensional flow. *Laminar boundary layers* 2(6), 72-82.

Liu, Y., J. Sun and L. Lu (2014). Corner Separation Control by Boundary Layer Suction Applied to a Highly Loaded Axial Compressor Cascade. *Energies*, 7(12): 7994-8007.

Merchant, A., A. Epstein and J. Kerrebrock (2004). Compressors with aspirated flow control and counter-rotation. *AIAA -2004-2514*.

Merchant, A., M. Drela, J. Kerrebrock, J. Adamczyk and M. Celestina (2000). Aerodynamic design and analysis of a high pressure ratio aspirated compressor stage. *ASME 2000-GT-619*.

Onnée, J. (2005). Aerodynamic performance measurements in a counter-rotating aspirated compressor. *Ph. D. thesis, the Massachusetts Institute of Technology, Boston, USA.*

Peacock, R (1971). Boundary-layer suction to eliminate corner separation in cascades of aerofoils. *HM Stationery Office*.

Qiang, X., W. Songtao, F. Guotai and W. Zhongqi (2008). Aerodynamic design and analysis of a low-reaction axial compressor stage. *Chinese Journal of Aeronautics*, 21(1),1-7.

Reijnen, D. (1997). Experimental study of

boundary layer suction in a transonic compressor. *Ph. D. thesis, the Massachusetts Institute of Technology, Boston, USA.*

Sachdeva, A and F. Leboeuf (2011). Topological Studies of Three-dimensional Flows in a High Pressure Compressor Stator Blade Row without and with Boundary Layer Aspiration. *Chinese journal of aeronautics* 24(5), 541-549.

Schuler, B (1998). Mechanical design of an experimental aspirated compressor. *Ph. D. thesis, the Massachusetts Institute of Technology, Boston, USA.*

Schuler, B., J. Kerrebrock and A. Merchant (2000). Design, analysis, fabrication and test of an aspirated fan stage. *ASME 2000-GT-618.*

Sinnettej, T. and G. Costello (1951). Possible Application of Blade Boundary-Layer Control to Improvement of Design and Off-Design Performance of Axial-Flow Turbomachines. *NACA Technical Note 2371.*

Song, Y., F. Chen, J. Yang and Z. Wang (2006). A numerical investigation of boundary layer suction in compound lean compressor cascades. *Journal of turbomachinery*, 128(2), 357-366.

Spalart, P. and S. Allmaras (1992). A One-Equation Turbulence Model for Aerodynamic Flows. *AIAA 92-0439.*

Wang, K (1972). Separation patterns of boundary layer over an inclined body of revolution. *AIAA Journal* 10(8), 1044-1050.

Zhang, H., S. Wang and Z. Wang (2007). Variation of vortex structure in a compressor cascade at different incidences. *Journal of propulsion and power* 23(1), 221-226.

Zhang, Y., A. Mahallati and M. Benner (2014). Experimental and Numerical Investigation of Corner Stall in a Highly-Loaded Compressor Cascade. *ASME GT2014-27204.*